Turk J Elec Engin, VOL.10, NO.2 2002, © TÜBİTAK

2D Complex Point Source Radiation Problem I. Complex Distances and Complex Angles

E. GAGO-RIBAS, M.J. GONZÁLEZ MORALES
Dpto. Teoría de la Señal y Comunicaciones e I.T., Universidad de Valladolid-SPAIN
e-mail: emigag@gbien.tel.uva.es
e-mail: chus@gbien.tel.uva.es

Abstract

A methodology based on the complex spaces analysis, which allows to generalize the study of wave radiation and scattering problems is presented in this paper. From the analytic continuation of functions defined in the real domain (real propagation or scattering spaces) into the complex space (space of complex coordinates), general non homogeneous phase field solutions are obtained for a particular wave problem. From these general solutions, other common solutions obtained under different approximations will arise. This procedure allows to obtain a complete classification of the solutions for the wave problem under analysis, and also to study both the ranges of validity of the different approximations, and the behavior of any particular solution, leading to a more general representation of the problem. In the present paper, the basis for this methodology will be presented in detail, and will be applied to the general complex beams wave propagation problem arising from the analytic continuation from homogeneous cylindrical waves and the corresponding free-space wave equation. As a direct consequence, new magnitudes arise from this formulation. Complex distances, complex angles and other complex magnitudes related to these are the essential ones. All of them are carefully analyzed in this first paper, mapping their meaning into the real propagation space, and emphasizing the interpretation of the results. All these magnitudes will play a fundamental role not only in the analysis of the radiation problem associated to a particular wave problem, but also in the later analysis of scattering problems involving non homogeneous general wave solutions (i.e. scattering problems under complex beams incidence). In this sense, the complex mappings presented in this paper will constitute the fundamental step to: (i) understand the general problem which involves all the particular solutions; (ii) characterize the behavior and ranges of validity of these particular solutions; (iii) understand the meaning of the complex magnitudes, such as complex distances and angles, and the information they can carry out into the real space in later practical problems such as scattering problems, and (iv) extend this methodology to represent other types of wave problems, such as those involving evanescent plane waves, surface waves, etc.

Key Words: *complex source, complex angle, complex beams, radiation, Green's function, propagation*

1. Introduction

The uniqueness in the definition of an analytic function establishes that *an analytic function is uniquely defined by its values on a certain set of points in the domain of its definition*, [1]. This circumstance allows to construct an analytic continuation of elementary functions of real variable into the complex domain and to elucidate their properties in this domain. Some consequences of the theory of complex functions are useful

tools for the analysis of boundary and initial value problems defined by partial differential equations, such as those for electromagnetic fields.

First publications with the idea of fixing a complex location are dated from the 60's. In 1964, Deschamps proposed to combine two real numbers which characterize a beam cross section into a single complex number, [2]. In 1967 and 1968 URSI meetings the same author gave some explanations to the fact of assigning a complex value to the location of a point-source in order to get a mathematical representation of Gaussian Beam solutions. Deschamps also formalized the idea of performing the analytic continuation of the Green's function into the complex space, [3].

In the 70's Felsen et al. start working in complex phase fields, [4–7], leading to the Evanescent Wave Tracking Theory (EWT). This theory was applied to several propagation, dispersion and guided waves problems, [4, 8–17].

In the 70's and 80's a lot of researchers were interested in Gaussian Beams and resolve hundreds of *specific* problems where beams were involved. Most of them were solved numerically, aided by the computers coming out with increasing numerical capabilities. These circumstances led to the analytical study of those problems be abandoned, sometimes neglecting elementary aspects such as the validity range of the usual approximations. We find a wide collection of representative problems. For instance, studies of the propagation in guided systems, [18], interface problems and stratified surfaces, [19, 20], radiation from apertures, reflection and diffraction by some representative structures [21, 22], diffraction by arrays, [23], or more recent studies dealing directly with the concept of complex distances applied to specific scattering problems, [24].

In the 90's Gago et al. starts again these topics in order to develop a complete analysis in the complex space, [25, 26]. These works try to make a formal parameterization of the usual approximations for complex point source fields, and to find out a physical interpretation for the whole set of solutions which appear from the complex point source location, [27, 28], starting with the analysis of complex magnitudes such as *complex distances* and some initial results related to *complex angles*, [29]. The general methodology is based on the analysis in the *complex spatial domain*; most calculations are performed in the complex domain and the results are translated or interpreted into the real spatial domain.

In the present paper, a complete study of the complex distances and complex angles spaces is presented in detail. The analysis is performed for the *particular* wave problem of continuing the *real homogeneous cylindrical wave solution* in a 2D free space problem, into a *general complex beam solution*, that covers a big amount of common particular solutions under different approximations (far field, high frequency, paraxial, etc.). The classification of the different solutions obtained for this particular problem is presented in this paper, while the analysis of the behavior of any solution as well as the different ranges of validity will be discussed in **Part II**.

From the beginning of these studies, it seemed for the authors that many of the analysis regarding the ranges of validity and behaviors of the different particular solutions should be performed directly from the general complex beam solution. This fact entitled to perform a careful analysis of the different complex magnitudes involved in the general complex beam solution, and also to translate these results into the real propagation space. As soon as a new solution in the general classification had to be studied, its analysis required to come back into the complex magnitudes planes associated to the problem; for instance, the *complex distances plane* played a fundamental role in the analysis of the real far field condition through the parameterization of the so called *complex radiation condition* (refer to section 2.2 in this paper). Also, in later scattering and diffraction problems currently under investigation (some initial results may be found in [30];

also, a paper with the first results obtained by applying this methodology is currently under preparation), the complex analysis turns up to new complex magnitudes and complex laws, i.e. the interpretation, after some asymptotic evaluation, of *complex rays*, *complex Snell law*, *complex Floquet modes*, etc. Once again, the complete understanding of these magnitudes required to analyze and interpret them into the corresponding complex magnitudes plane, i.e. the *space of complex angles* and the complex trigonometric functions associated to them. Even more, the parameterization and interpretation of the space of complex angles also required the previous analysis of the space of complex distances as well. As a result of this *back to basis* process, a important set of complex mappings and their real space interpretation was performed (refer to Section 3 for complex distances, and Section 4 for complex angles, both in the present paper); the current classification of these mappings and their particular interpretation constitute the main objective of the present first paper.

Up to our knowledge, the importance of the analysis of these complex spaces is related not only to the particular aspects concerning the complex beam problem presented in these two papers, but also due to the general information that lies into them. In first place, their analysis provide general information to describe other kinds of wave propagation problems; i.e. the space of complex angles provided important information to characterize different kinds of evanescent waves, such as *evanescent plane waves* and *surface waves*, [30]. Also, the usual relationships between the real space vector $\vec{r}$, and the real wave number vector $\vec{k}$, both related to real distances, real angles and real spectral representations, turn up to investigate new important mathematical properties associated to complex $\vec{\mathbf{r}}$ spaces and complex wave number $\vec{\mathbf{k}}$ spaces, both related to *complex distances*, *complex angles* and *complex spectral representations*. Finally, a set of new interesting mathematical problems and their application to generalize wave propagation solutions appear from these initial complex analyses; for instance, the generalization of the theory of distributions or generalized functions in the complex space. These problems and their possible application to the representation of wave propagation phenomena is currently under study by the authors.

2. Mathematical Representation of the Problem

2.1. Mathematical formulation

Let us assume the space geometry depicted in Figure 1. The problem is defined in a 2D space assuming invariance along the $y-$direction. Time-harmonic dependence in the form $e^{-i\omega t}$ will be assumed and dependence in the wavenumber domain will be in the form e^{ikr}. Let us consider the unit line source located at (x_s, z_s). The observation point and the source position vectors are represented by $\vec{r}$ and $\vec{r}_s$ respectively, with $k_0 = \omega\sqrt{\mu_0\epsilon_0}$ denoting the free space wavenumber.

The scalar 2D free space Green's function is defined by the wave equation,

$$\left(\nabla^2 + k_0^2\right) G_f(\vec{r}, \vec{r}_s) = -\delta(\vec{r}, \vec{r}_s) \tag{1}$$

which solution is the well-known Hankel function of zero order and first kind [1]

$$G_f(\vec{r}, \vec{r}_s) = \frac{i}{4} H_0^{(1)}(k_0|\vec{r} - \vec{r}_s|) = \frac{i}{4} H_0^{(1)}(k_0 R_s) \tag{2}$$

with

$$R_s = |\vec{r} - \vec{r}_s| = \sqrt{(x - x_s)^2 + (z - z_s)^2} \tag{3}$$

[1] A time dependence in the form $e^{-i\omega t}$ leads to $H_0^{(1)}$ solution while a time dependence $e^{j\omega t}$ leads to $H_0^{(2)}$ solution.

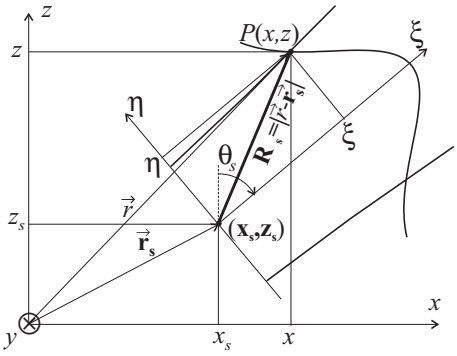

Figure 1. 2D free space radiation problem. Complex source point.

denoting the *real distance* from the source position to the observation point. By performing the analytic continuation from the real coordinates of the source into the complex space,

$$\begin{aligned} \mathbf{x_s} &= x_s + ib\sin\theta_s \\ \mathbf{z_s} &= z_s + ib\cos\theta_s; \qquad b > 0, \end{aligned} \tag{4}$$

a new **complex Green's function** is obtained.

$$G_f(\vec{r},\vec{\mathbf{r}}_\mathbf{s}) = \frac{i}{4}H_0^{(1)}(k_0|\vec{r}-\vec{\mathbf{r}}_\mathbf{s}|) = \frac{i}{4}H_0^{(1)}(k_0\mathbf{R_s}) \tag{5}$$

with,

$$k_0\mathbf{R_s} = |\vec{r}-\vec{\mathbf{r}}_\mathbf{s}| = \sqrt{(x-\mathbf{x_s})^2+(z-\mathbf{z_s})^2}. \tag{6}$$

Because of the added imaginary part is a constant, the new function with a complex argument is also a valid solution of the original wave equation, [5, 7]. This may be proved because the imaginary part is not affecting the partial derivates of the differential equation. The complex position vector of the source will be denoted by $\vec{\mathbf{r}}_\mathbf{s}$ while the real observation points will constitute the *Real Propagation Space* (RPS). The resulting analytically continued magnitude $\mathbf{R_s}$ obtained from R_s will be referred as *complex distance*, from the real observation point to the complex position of the source and will define the *Space of Complex Distances* (SCD). From the complex-point source definition, it is also possible to define a *complex angle* in a similar way to real angles. For instance, from the *tangent* trigonometric function we may define, in the general (x, z) coordinate system,

$$\tan\boldsymbol{\theta} = \frac{x-\mathbf{x_s}}{z-\mathbf{z_s}}. \tag{7}$$

The complex angles analysis will introduce a representation for the field characteristics which will allow both, energy propagation direction and field attenuation interpretations. This magnitude will be very important in the analysis of complex scattering problems, as well as other wave solutions not presented here, for instance, evanescent plane waves and complex surface waves, [30]. The original complex angle or its corresponding complex trigonometric relationships will define complex spaces such as the *Space of Complex Angles* (SCA), the *Space of the Tangent of a Complex Angle* (STCA), the *Space of the Sine of a Complex Angle* (SSCA) and the *Space of the Cosine of a Complex Angle* (SCCA).

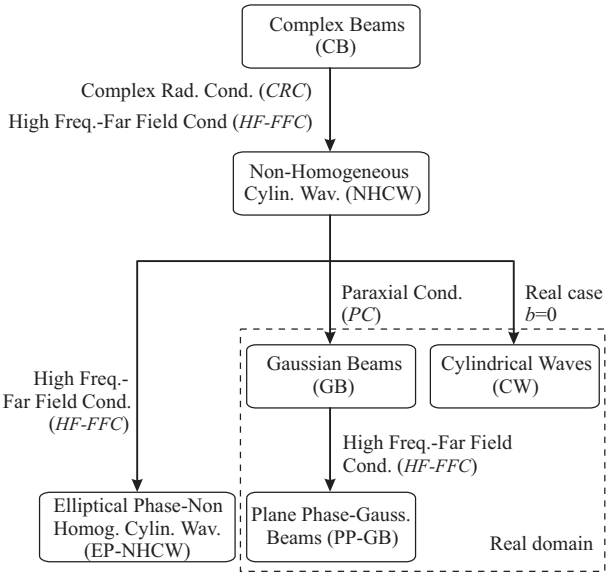

Figure 2. Summary of the approximations and associated solutions.

By performing a change of variables, shifting and rotating the Cartesian coordinates an angle θ_s, the coordinates centered on the beam axis[2] (ξ, η) as shown in Figure 1 are obtained. This rotation angle will parameterize the beam incidence angle when being applied to scattering problems. The following relationships may be obtained:

$$\begin{aligned} x - x_s &= \xi \sin\theta_s - \eta \cos\theta_s, \\ z - z_s &= \xi \cos\theta_s + \eta \sin\theta_s, \end{aligned} \tag{8}$$

$$\begin{aligned} \xi &= +(x - x_s)\sin\theta_s + (z - z_s)\cos\theta_s, \\ \eta &= -(x - x_s)\cos\theta_s + (z - z_s)\sin\theta_s. \end{aligned} \tag{9}$$

Thus, the complex distance in terms of the new coordinate system may be written as

$$\mathbf{R_s} = \sqrt{(\xi - ib)^2 + \eta^2} = \sqrt{\xi^2 + \eta^2 - b^2 - i2b\xi}, \tag{10}$$

and the complex angle becomes $\boldsymbol{\theta_c}$,

$$\tan\boldsymbol{\theta_c} = \frac{\eta}{\xi - ib}. \tag{11}$$

By replacing (10) into (5), a set of different field solutions presenting beam characteristics are obtained. The analysis of these field solutions is made in **Part II** and summarized in next section.

2.2. Summary of the solutions

A brief summary of all the solutions and approximations is made in Figure 2.

[2]It will be shown that ξ is the usual beam axis.

Starting from the exact solution in (2) named as *Complex Beams* (CB's), by applying the asymptotic condition, or its complex version named as *Complex Radiation Condition* (*CRC*), the *Non Homogeneous Cylindrical Waves* (NHCW's) are obtained. By assuming the CRC and applying the *Paraxial Condition* (*PC*), the *Gaussian Beams* (GB's) are obtained. Both NHCW and GB solutions present a dominant phase term coming from a exponential term (ET) in the form $e^{ik_0\mathbf{R_s}}$, which makes possible to neglect contributions from the square root terms under *High Frequency-Far Field Condition* (*HF-FFC*), leading to *Elliptical Phase-Non Homogeneous Cylindrical Waves* (EP-NHCW) and *Plane Phase-Gaussian Beams* (PP-GB) solutions, respectively. By cancellation of the imaginary parts of the complex coordinates, the original Cylindrical Wave (CW) solution is obtained. The CW, GB and PP-GB solutions are susceptible of a real analysis; the CW's because they have homogeneous phase in fact, and the GB's because, even if they have geneous phase, the complex phase is easily separated into real and imaginary parts, allowing the analysis in the real space. In **Part II** of this work the field behavior for all these solutions will be analyzed by using the complex parameterization of the different approximations.

3. Space of Complex Distances

3.1. Definition

The parameterization of the RPS in terms of the SCD was described in [26] and only a brief summary will be presented here. The basis of the analysis will be the complex function $\mathbf{R_s}$ in (10).

3.2. Selected curves of special interest

A list of curves have been selected to be studied in detail because of some characteristic which make them to have a special relevance in radiation or scattering problems as mentioned in the introduction. Some of them are defined from its distinguishing feature in the RPS and will mapped into all complex spaces. Other ones are defined in the SCD and will be mapped into the RPS and also into the complex spaces related to complex angles.

- Real ξ axis (labeled as 1 in Figure 3): It will be shown that it is not only an axis of the coordinate system in the RPS but also the boundary of the valid mapped regions in all the complex spaces as shown in Figure 4. It will be also seen that all the complex magnitudes degenerate into this real axis far away from the source in relation to parameter b, or when $b \to 0$.

- Real η axis (labeled as 2 in Figure 3): We will distinguish two cases: $|\eta| \leq b$ and $|\eta| \geq b$, which will be labeled as 2a and 2b, respectively. We will see that these lines also limit the boundary of the valid mapped regions in most of the complex spaces as shown in Figure 4.

- Phase paths for the ET, $v = v_c$ (labeled as 3 in Figure 3): In the analysis of the field solutions in **Part II**, we will place a special emphasis in the ET appearing in the NHCW expression $e^{ik_0\mathbf{R_s}}$. The phase paths of this field contribution are defined in the SCD by these curves.

- Phase fronts for the ET, $u = u_c$ (labeled as 4 in Figure 3): This curves are also defined in the SCD. They describe the phase fronts of the ET field contribution.

- Circumferences on the RPS (labeled as 5 in Figure 3): They describe the real distance between any observation point and the real location of the source. We will distinguish three cases: $R_s < b$, $R_s = b$ and $R_s > b$ which will be labeled as 5a, 5b and 5c, respectively.
- Circumferences on the SCD (labeled as 6 in Figure 3): The curves of constant error of the *CRC*, Figure 2, are defined in the SCD and are circumferences with $k_0|\mathbf{R_s}| = \rho_{CRC}$. These curves define the boundary regions where the NHCW approximation is valid for a fixed error.
- Paraxial limit established by the *PC* (labeled as 7 in Figure 3): The distinguishing feature of these curves is that they limit the boundary of the paraxial condition. They are defined in the RPS by hyperbolas described by $\eta^2 = (\xi^2 + b^2)/\rho_{PC}^2$.
- Radial lines on the RPS (labeled as 8 in Figure 3): They define straight directions departing from the real source location on the RPS and are also the asymptotes of the phase paths for the ET and the paraxial condition.

All these curves will be mapped into all the complex spaces studied in next sections, providing with a good idea of the important properties associated to the complex analysis.

3.3. Summary of the transformations

3.3.1. Real propagation space

In Figure 3a, all the curves of special interest are represented on the RPS. Some of these curves were defined on the RPS and some were originally defined on the SCD. The corresponding translation from the RPS into the SCD or vice versa was also performed. In order to parameterize the transformation from the RPS (ξ, η) to the SCD (u, v) with $\mathbf{R_s} = u + iv$, we will use the auxiliary space of the square complex distances $\mathbf{R_s^2}$.

3.3.2. Space of square complex distances

Let us call $\mathbf{R_s^2} = \mathbf{z} = z_1 + iz_2$. In terms of (ξ, η) it may be written as

$$\begin{aligned} z_1 &= \xi^2 + \eta^2 - b^2, \\ z_2 &= -2b\xi. \end{aligned} \tag{12}$$

In Figure 3b, all the curves of special interest on the wavenumber-scaled complex plane $k_0^2\mathbf{R_s^2}$ are shown.

3.3.3. Space of complex distances

The SCD, $\mathbf{R_s}$ may be obtained from the $\mathbf{z}$ plane by using the complex transformation $\mathbf{R_s} = \sqrt{\mathbf{z}} = u + iv$. The appropriate root solution must be chosen to satisfy the physical conditions of the problem. The physical meaning of the complex distance is found by substituting its value on the original Green's function in (5),

$$G_f \sim \frac{e^{i\pi/4}}{2\sqrt{2\pi}} \frac{e^{ik_0\mathbf{R_s}}}{\sqrt{k_0\mathbf{R_s}}} = \frac{e^{i\pi/4}}{2\sqrt{2\pi}} \frac{e^{-k_0 v} e^{ik_0 u}}{\sqrt{k_0\mathbf{R_s}}}. \tag{13}$$

For the selected time-harmonic variation, condition $\Re\{\mathbf{R_s}\} = u > 0$ must be imposed in order to obtain outgoing waves, and condition $\Im\{\mathbf{R_s}\} = v < 0$ must be imposed in order to satisfy the radiation condition

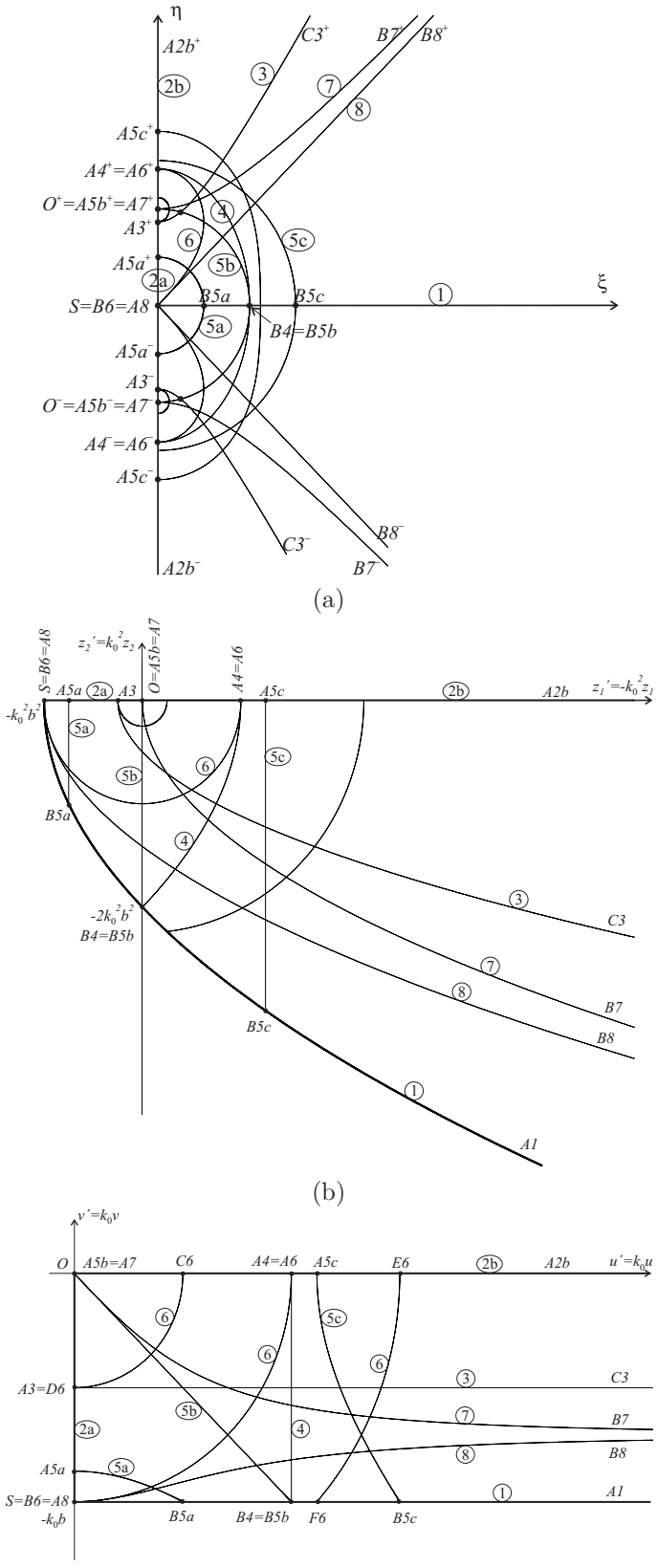

Figure 3. Summary of some curves of special interest represented: (a) in the RPS, (b) in the square SCD, and (c) in the SCD.

at infinity in the semi-plane $\xi > 0$. With these considerations in mind, the relations of (u, v) in terms of (z_1, z_2) are given by,

$$\begin{aligned} u &= \frac{1}{\sqrt{2}}\sqrt{|\mathbf{z}| + z_1} = \frac{1}{\sqrt{2}}\sqrt{\sqrt{z_1^2 + z_2^2} + z_1}, \\ v &= \frac{-1}{\sqrt{2}}\sqrt{|\mathbf{z}| - z_1} = \frac{-1}{\sqrt{2}}\sqrt{\sqrt{z_1^2 + z_2^2} - z_1}. \end{aligned} \tag{14}$$

From (12), the relations of (u, v) in terms of (ξ, η) may be obtained straight forward, leading to,

$$\begin{aligned} u &= \frac{1}{\sqrt{2}}\sqrt{\sqrt{(\xi^2 + \eta^2 - b^2)^2 + 4b^2\xi^2} + \xi^2 + \eta^2 - b^2}, \\ v &= -\frac{1}{\sqrt{2}}\sqrt{\sqrt{(\xi^2 + \eta^2 - b^2)^2 + 4b^2\xi^2} - (\xi^2 + \eta^2 - b^2)}. \end{aligned} \tag{15}$$

In Figure 3c, all the curves of special interest on the wavenumber-scaled complex plane $k_0\mathbf{R_s}$ are shown. From these relations, the corresponding *inverse* transformations $(u, v) \to (z_1, z_2) \to (\xi, \eta)$ may also be obtained,

$$\begin{aligned} z_1 &= u^2 - v^2, \\ z_2 &= 2uv, \end{aligned} \tag{16}$$

and,

$$\begin{aligned} \xi &= -\frac{z_2}{2b}, \\ \eta &= \pm\sqrt{z_1 - \left(\frac{z_2}{2b}\right)^2 + b^2}. \end{aligned} \tag{17}$$

The final relation between the SCD and the RPS may be summarized by

$$\begin{aligned} \xi &= -\frac{uv}{b}, \\ \eta &= \pm\sqrt{u^2 - v^2 - \frac{u^2v^2}{b^2} + b^2}. \end{aligned} \tag{18}$$

From this general relations, the curves of special interest may be analytically obtained in these three representative planes. The particular expressions for each curve are detailed in [26, 30] and summarized in Figure 3.

3.4. Interpretation of the results

Some important observations may be extracted from the analysis of these results.

- The root selection and, in consequence, the SCD validity range depends on the field solution which is under analysis. The real axes $(\xi = 0, \eta = 0)$ and their mapped curves into the SCD will determine the boundary regions on any space. This fact is summarized in Figure 4. The source location described by parameter b has a fundamental relevance in the mappings.

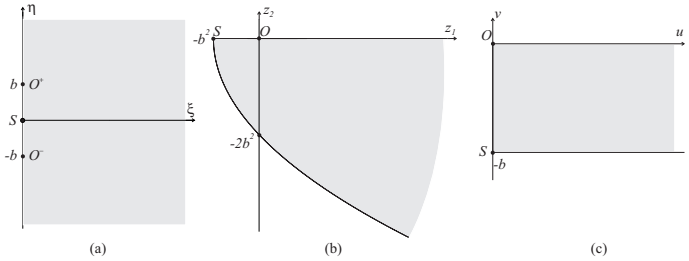

Figure 4. Complex spaces validity regions: (a) RPS, (b) Square SCD, and (c) SCD.

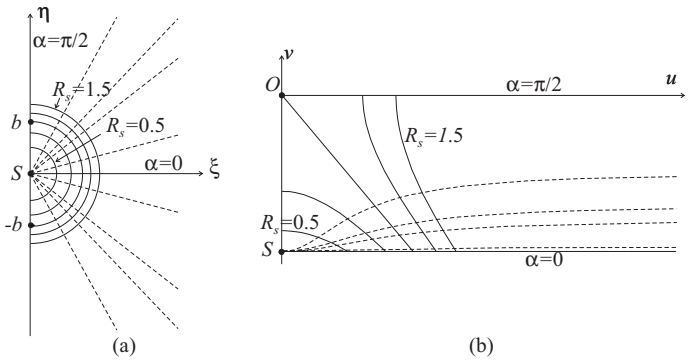

Figure 5. Real distances and real directions parameterization: (a) in the RPS, and (b) in the SCD. Example with $b = 1$, $R_s = 0.5, 0.7893, 1, 1.1735, 1.3229, 1.5$ and $\alpha = 0.2450, 0.6435, \pi/4, \pi/3$ radians.

- A complete parameterization of the SCD has been obtained by mapping the most representative and useful curves in both, the SCD and the RPS. The parametric relations allow to map any curve from one space to another, and to understand the behavior or dependence with any parameter, such as b or k_0. For instance, Figure 5 shows some curves describing both, constant real distances and constant real directions; their representation on the SCD is also shown.

- Complex point S with coordinates $(u = 0, v = -b)$ in the SCD is mapped into $(\xi = 0, \eta = 0)$ in the RPS, and point O with coordinates $(u = 0, v = 0)$ is mapped into points $(\xi = 0, \eta = \pm b)$. The complex source may be interpreted as the straight line $(\xi = 0, -b \leq \eta \leq b)$ in the RPS.

- The SCD analysis also reveals the behavior of the ET. In **Part II**, it will be found that the ET represents the main contribution to the NHCW field solution. Curves with constant $v = v_c$ are the curves with constant amplitude of the field, and curves with constant $u = u_c$ describe the phase fronts of the field solution. The consequence of the orthogonal condition of these sets of curves in both, the SCD and the RPS, is that the constant amplitude curves are identical to the phase paths. This fact is schematized in Figure 6.

- The *CRC* parameterization is a representative example of the advantage and utility of the SCD analysis. The boundary between the exact CB solution and the asymptotic NHCW solution is represented in the RPS and the SCD, parameterized in terms of b and k_0, and depending on ρ_{CRC} parameter. A similar analysis is made for the *PC* and the boundary of the NHCW solution and the paraxial GB solution: parameterization in terms of b, k_0 and ρ_{PC}. By combining *CRC* and *PC* conditions, scenarios as those in Figure 7 will be found.

- From Figure 7, surprising observations about *real/complex distances* and *near/far field* from the

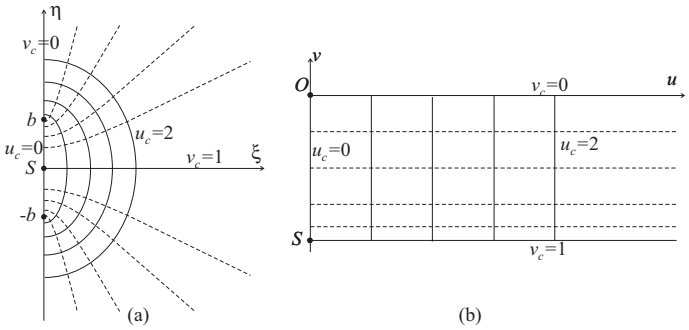

Figure 6. Constant amplitude curves and phase fronts for the exponential term. The constant amplitude curves are identical to the phase paths: (a) in the RPS; (b) in the SCD. Example with $b = 1$, $u_c = 0, 0.5, 1, 1.5, 2$ and $v_c = 0, 0.25, 0.5, 0.75, 0.9, 1$.

complex source are found out. For instance, when $\rho_{CRC}/k_0 = 0.5$, the real location of the source, point S, is located in the far field region, and it is possible to extend the validity range of the NHCW approximation into nearly the whole RPS.

- Once the relations between the spaces $(\xi, \eta) \leftrightarrow (z_1, z_2) \leftrightarrow (u, v)$ are established, they may be applied to map any relevant curve such as the boundaries of associated to the *HF-FFC* approximations already suggested in Figure 2.

4. Space of Complex Angles

4.1. Definition

From the scenario shown in Figure 8, it is possible to define a complex angle $\boldsymbol{\theta_c}$ with respect to the beam axis, using the following relationships:

$$\tan \boldsymbol{\theta_c} = \frac{\eta}{\xi - ib}, \tag{19}$$

$$\sin \boldsymbol{\theta_c} = \frac{\eta}{\mathbf{R_s}}, \tag{20}$$

$$\cos \boldsymbol{\theta_c} = \frac{\xi - ib}{\mathbf{R_s}}. \tag{21}$$

A more general complex angle $\boldsymbol{\theta}$ may be defined with respect to an arbitrary direction, which will be fixed to z axis, in the general (x, z) coordinate system, using the following relations:

$$\tan \boldsymbol{\theta} = \frac{x - \mathbf{x_s}}{z - \mathbf{z_s}}, \tag{22}$$

$$\sin \boldsymbol{\theta} = \frac{x - \mathbf{x_s}}{\mathbf{R_s}}, \tag{23}$$

$$\cos \boldsymbol{\theta} = \frac{z - \mathbf{z_s}}{\mathbf{R_s}}. \tag{24}$$

Any of them may be used to define the SCA. In fact, it may be easily found that,

$$\boldsymbol{\theta} = \theta_s - \boldsymbol{\theta}_c, \tag{25}$$

with $\boldsymbol{\theta_c}$ being a particular case of $\boldsymbol{\theta}$. When $\theta_s = 0$, the relation reduces to $\boldsymbol{\theta} = -\boldsymbol{\theta_c} = -\Re\{\boldsymbol{\theta_c}\} - i\Im\{\boldsymbol{\theta_c}\}$[3].

The angle $\boldsymbol{\theta_c}$ has been defined centered with respect to the beam axis. On the other hand, $\boldsymbol{\theta}$ is a more general angle with respect to an arbitrary direction. This definition arises by keeping in mind the most convenient way to be applied later to scattering problems. For instance, if the scatter is on x'-axis, parallel to x, Figure 8, the incident angle will be $\boldsymbol{\theta}$ as it was previously defined.

Once one of the complex magnitudes in (19)-(24) is obtained, the related ones may be mathematically obtained straight forward by applying trigonometric relations. The goal of this study is not to get the value of these magnitudes for any observation point, but it is to find out the most convenient parameterization in order to understand how this magnitudes behave, particularly over some curves which have a special relevance to reveal the information they involve about the description of the physical behavior of any field solution.

4.2. Summary of the transformations

4.2.1. Tangent of a complex angle

The tangent of a complex angle in (19) defined from ξ-axis,

$$\tan \boldsymbol{\theta_c} = \frac{\eta\xi}{\xi^2 + b^2} + i\frac{\eta b}{\xi^2 + b^2}. \tag{26}$$

The complex space $\tan(-\boldsymbol{\theta_c})$ may be obtained as $-\tan \boldsymbol{\theta_c} = -\Re\{\tan \boldsymbol{\theta_c}\} - i\Im\{\tan \boldsymbol{\theta_c}\}$. Thus, the first quadrant ($\eta > 0$) and the third quadrant ($\eta < 0$) should be interchanged each other.

The tangent of a complex angle turned from the beam axis defined in (22) or STCA, may be obtained from the auxiliary spaces $\mathbf{n} = n_1 + in_2 = x - \mathbf{x_s}$ and $\mathbf{d} = d_1 + id_2 = z - \mathbf{z_s}$. Let us call $\tan \boldsymbol{\theta} = \mathbf{n}/\mathbf{d} = t_1 + it_2$; the final following relations may be obtained,

$$\begin{aligned} t_1 &= \frac{n_1 d_1 + n_2 d_2}{d_1^2 + d_2^2}, \\ t_2 &= \frac{n_2 d_1 - n_1 d_2}{d_1^2 + d_2^2}. \end{aligned} \tag{27}$$

The transformation of the curves of special interest into the STCA are plotted in Figure 9(a), by using the same labels as in Figure 3.

4.2.2. Sine of a complex angle

To deal with the SSCA analysis defined by (23), the auxiliary spaces $\mathbf{w} = 1/\mathbf{R_s}$ and $\mathbf{n} = x - \mathbf{x_s}$ may be used. Thus, $\sin \boldsymbol{\theta} = \mathbf{nw} = s_1 + is_2$ will lead to the following relations,

$$\begin{aligned} s_1 &= n_1 w_1 - n_2 w_2, \\ s_2 &= n_1 w_2 + n_2 w_1. \end{aligned} \tag{28}$$

All the curves of special interest in the SSCA are also summarized in Figure 9(b).

[3]The minus sign is because when $\theta_s = 0$, $\hat{x} = -\hat{\eta}$.This comes from the definition of the complex source in (4).

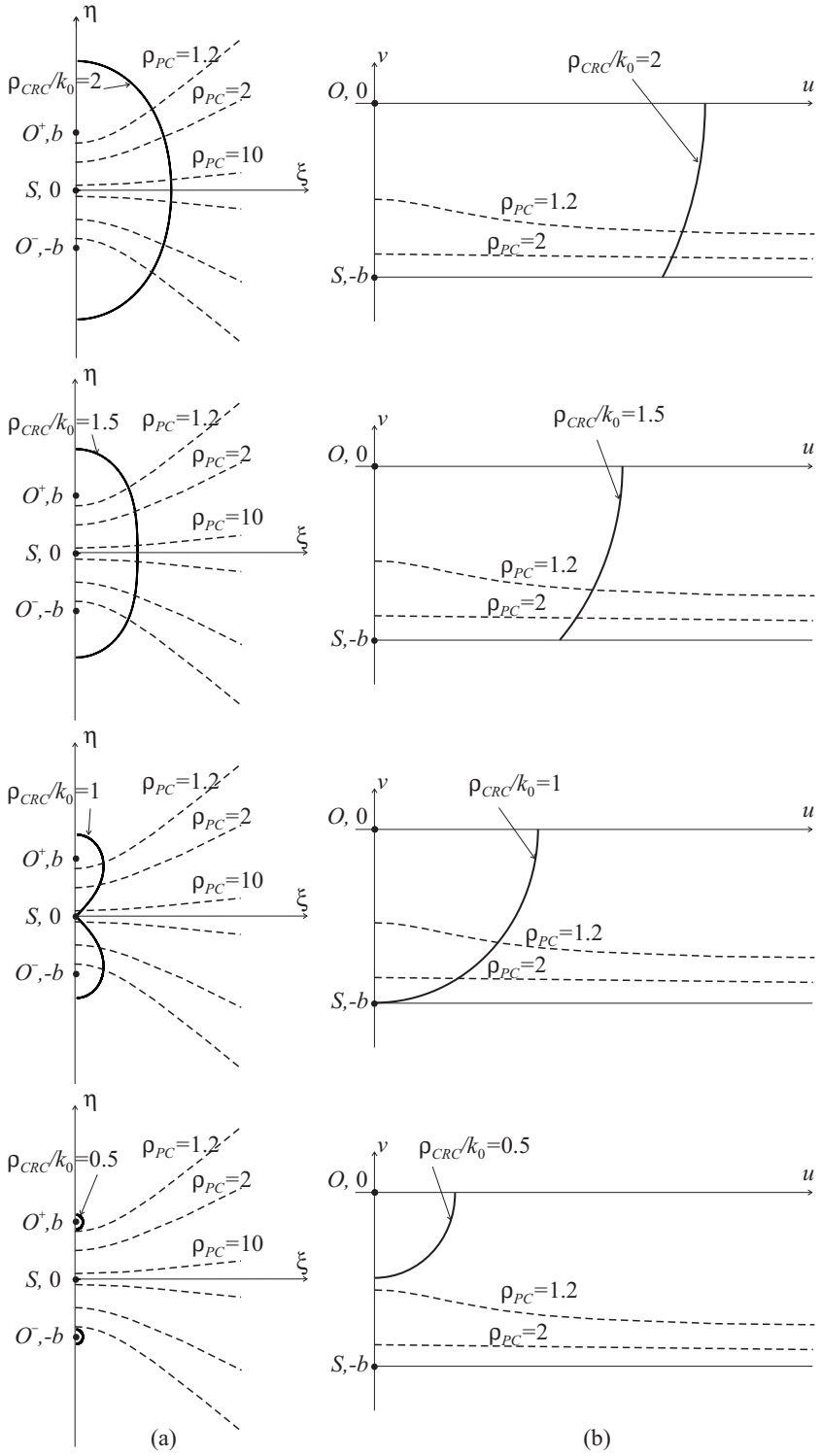

Figure 7. *CRC* and *PC* parameterizations: (a) in the RPS, and (b) in the SCD.

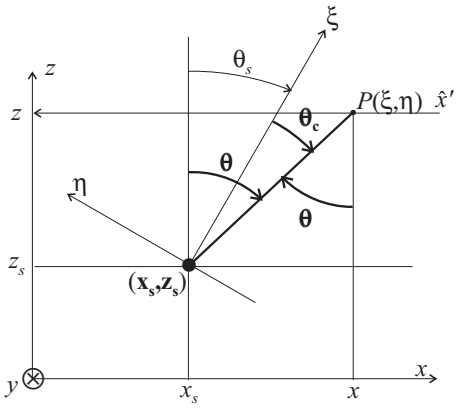

Figure 8. Definition of a complex angle. $\boldsymbol{\theta}_c$ is defined from $\hat{\xi}$ direction and $\boldsymbol{\theta}$ is defined from an arbitrary direction $\hat{z}$, shifted a real angle θ_s from the ξ axis.

4.2.3. Cosine of a complex angle

The SCCA defined in (24) may be obtained in a similar way as $\sin\boldsymbol{\theta}$, by using the auxiliary spaces $\mathbf{d} = z - \mathbf{z_s}$ and $\mathbf{w} = 1/\mathbf{R_s}$. Thus, $\cos\boldsymbol{\theta} = \mathbf{dw} = c_1 + ic_2$; the final relations are then given by,

$$\begin{aligned} c_1 &= d_1 w_1 - d_2 w_2, \\ c_2 &= d_1 w_2 + d_2 w_1. \end{aligned} \tag{29}$$

All the curves of special interest maybe obtained from these parametric relations. The results are plotted in Figure 9c.

4.2.4. Space of complex angles

The complex angle $\boldsymbol{\theta_c}$ may be obtained from the inverse trigonometric functions, $\tan^{-1}$, etc. It has a easy interpretable signification (i) for ξ- and η-axis, where specially simple expressions may be analytically found, and (ii) far away from the source where the imaginary part vanishes. For a general observation point, the complex angle value needs to be obtained numerically, but it provides with a very valuable information which will be detailed in next section.

The general complex angle defined from an arbitrary direction $\boldsymbol{\theta}$ may also be obtained from the inverse trigonometric functions. All the curves of special interest were numerically found and are plotted in Figure 10. The complex $\boldsymbol{\theta}$-plane is the same as $\boldsymbol{\theta_c}$-plane inverted and with a *displacement* of θ_s. This results fit with the relation in (25), and makes the analysis of $\boldsymbol{\theta}_c$ good enough for some purposes.

4.3. Interpretation of the results

Some conclusions may be extracted from the analysis of the results in last section.

- It is important to remark that the conventional trigonometric relationships hold. For instance, the Euler formula, $\sin^2\boldsymbol{\theta} + \cos^2\boldsymbol{\theta} = 1$, makes possible to write relations such as $\mathbf{R_s} = (\eta\sin\boldsymbol{\theta_c} + (\xi - ib)\cos\boldsymbol{\theta_c})$.

- Complex angles have been defined through their trigonometric functions. Any point in the RPS will be related to a specific point in the SCA, but this is not a conformal mapping and there is not a one-to-one

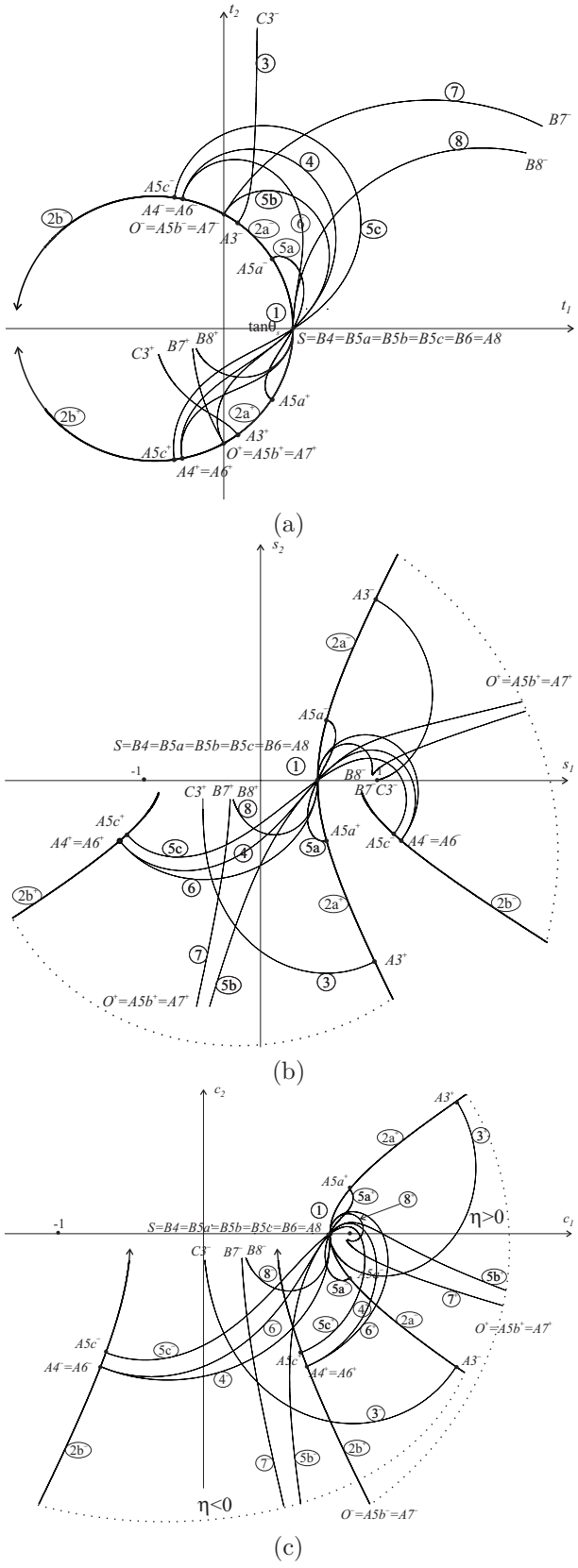

Figure 9. Trigonometric functions of a complex angle turned from the ξ axis a real angle $\theta_s = \pi/6$: (a) STCA $\tan \boldsymbol{\theta}$, (b) SSCA $\sin \boldsymbol{\theta}$, and (c) SCCA $\cos \boldsymbol{\theta}$.

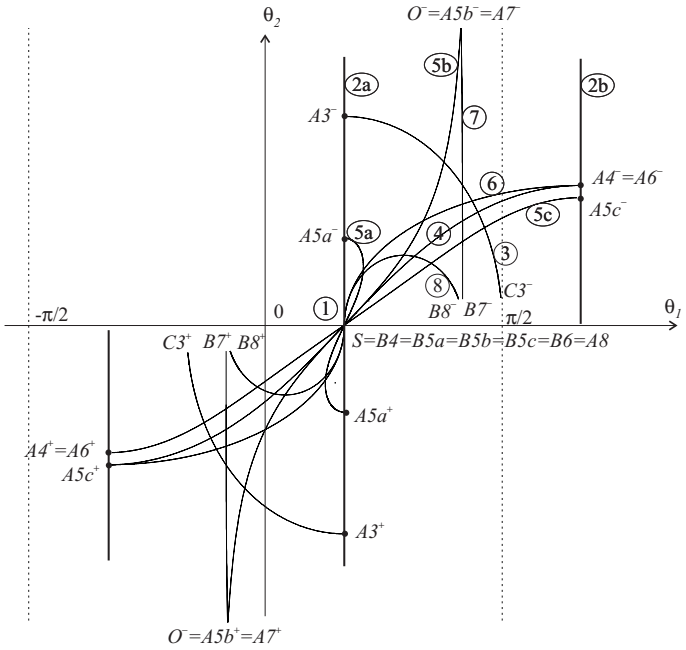

Figure 10. Summary of the curves of special interest in the SCA.

transformation. For instance, all the points belonging to the real ξ-axis have the same mapped point into the SCA.

- The $\boldsymbol{\theta_c}$-plane is easier to study than $\boldsymbol{\theta}$ because its trigonometric functions have simpler expressions. These two planes are related by just a horizontal displacement.

- The SCA related to $\boldsymbol{\theta}$ is the most convenient magnitude in order to find out the physical meaning of a complex angle, the relationship to the real propagation space, and the propagation characteristics of the fields as will be next discussed. Also, the SSCA and SCCA related to $\sin\boldsymbol{\theta}$ and $\cos\boldsymbol{\theta}$ are the most convenient spaces to handle reflection, scattering or diffraction problems and the laws associated to these processes. Some simple scattering problems are being currently investigated, [30,31], by means of a complete analysis in the *complex space domain*. The complex angle formulation will be a powerful tool in order to understand, for instance, the *complex Snell* and the *complex Floquet laws* interpretations.

- A complete parameterization of the RPS into the SCA has been performed. The most interesting curves have been mapped in terms of k_0 and b parameters. The parametric relations allow to add any other curve of interest straight forward. In Figure 11, the parameterization in terms of the real distance and the real direction is shown. In Figure 12, the parameterization of the phase fronts and phase paths for the ET is shown.

- In Figures 13 and 14, two examples of the dependence with θ_s are represented. From the observation of the case $\theta_s = \pi/18$, by making $\theta_s \to 0$, an intuitive vision of the $\boldsymbol{\theta_c}$ behavior is induced, which may be checked in the formulation. From the comparison of $\theta_s = \pi/3$ and $\theta_s = \pi/6$ cases, some symmetrical and periodic properties, related to complex trigonometric functions, are visualized.

- The following particular cases have an easy interpretation: (i) All trigonometric magnitudes become real on the ξ-axis and their value fits to the *real case* when $b = 0$; (ii) On the η-axis with $|\eta| \leq b$,

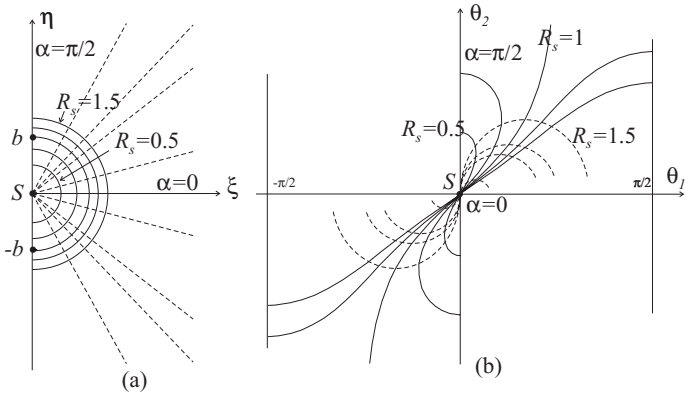

Figure 11. Real distances and real directions parameterization: (a) in the RPS, and (b) in the SCA. Example with $b = 1$, $R_s = 0.5, 0.7893, 1, 1.1735, 1.3229, 1.5$ and $\alpha = 0.2450, 0.6435, \pi/4, \pi/3$ radians.

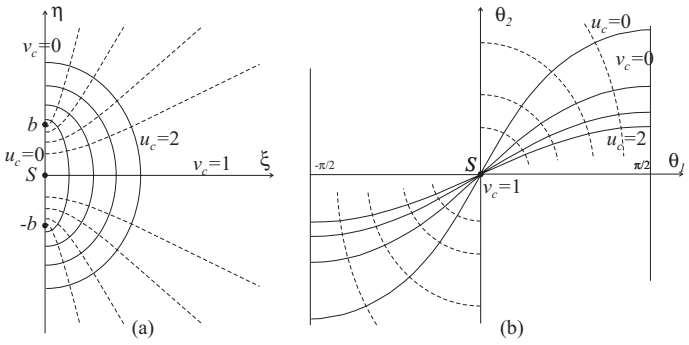

Figure 12. Exponential term phase fronts and phase paths parameterization: (a) in the RPS, and (b) in the SCA. Example with $b = 1$, $u_c = 0, 0.5, 1, 1.5, 2$ and $v_c = 0, 0.25, 0.5, 0.75, 0.9, 1$.

(curve 2a), the real part of the complex angle is identical to the value on the ξ-axis. Imaginary part increases as long as $|\eta| \to b$. On the η-axis with $|\eta| \geq b$, (curve 2b), the real part of the complex angle is shifted $\pi/2$ with respect to the value on the ξ-axis. Imaginary part increases as long as $|\eta| \to b$ and vanishes when $|\eta| \to \infty$, and (iii) Points far away from the source $R_s \to \infty$ or $R_s \gg b$, (curve 5c), have $\theta_2 \to 0$ and the imaginary part of all these magnitudes vanishes.

- **Complex angle interpretation.** By studying the ET phase fronts and phase paths, Figure 12, comparing the points in the RPS with the amplitude and phase values of the ET, Figure 15, and assuming that the main contribution to the field under study is $e^{ik_0\mathbf{R_s}} = e^{ik_0(\eta \sin \boldsymbol{\theta_c} + (\xi - ib)\cos \boldsymbol{\theta_c})}$, the following interesting conclusions maybe extracted about the real interpretation of the complex angle.

- **The real part of the complex angle**, Figure 17a, provides with the information about the propagation direction of the ET. By calling,

$$\tan \theta_{ET} = \frac{d\eta}{d\xi} = \frac{\eta\xi}{\xi^2 + v_c^2}, \tag{30}$$

as defined in Figure 16, it may be concluded that

$$\theta_{ET} = \Re\{\boldsymbol{\theta_c}\}. \tag{31}$$

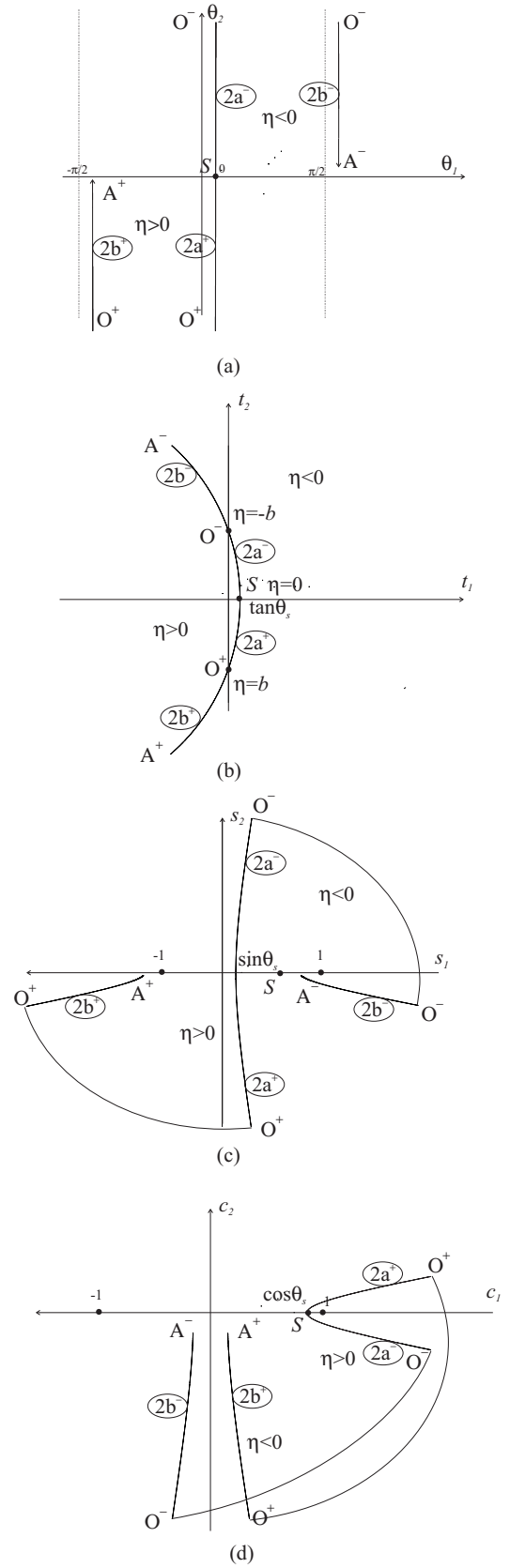

Figure 13. Complex spaces related to the SCA when $\theta_s = \pi/18$: (a) SCA; (b) STCA; (c) SSCA, and (d) SCCA. Reference points: $\mathrm{O}^{\pm}(\xi = 0, \eta = \pm b)$, $\mathrm{A}^{\pm}(\xi = 0, \eta = \pm\infty)$ and source $S(\xi = 0, \eta = 0)$.

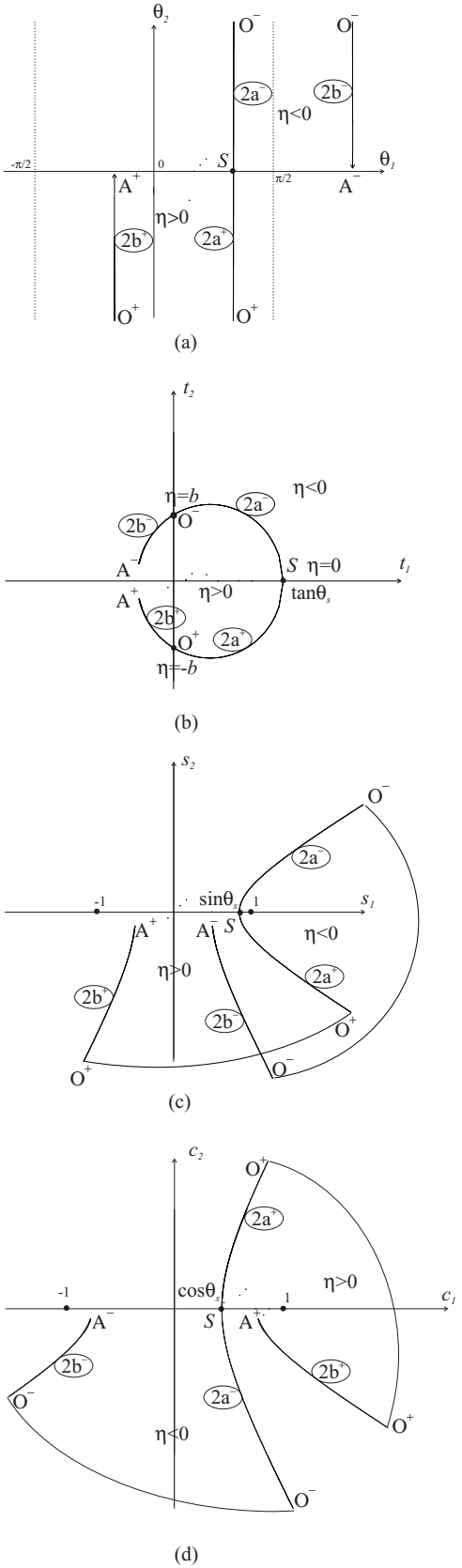

Figure 14. Complex spaces related to the SCA when $\theta_s = \pi/3$: (a) SCA; (b) STCA; (c) SSCA, and (d) SCCA. Reference points: $\mathrm{O}^{\pm}(\xi = 0, \eta = \pm b)$, $\mathrm{A}^{\pm}(\xi = 0, \eta = \pm\infty)$ and source $S(\xi = 0, \eta = 0)$.

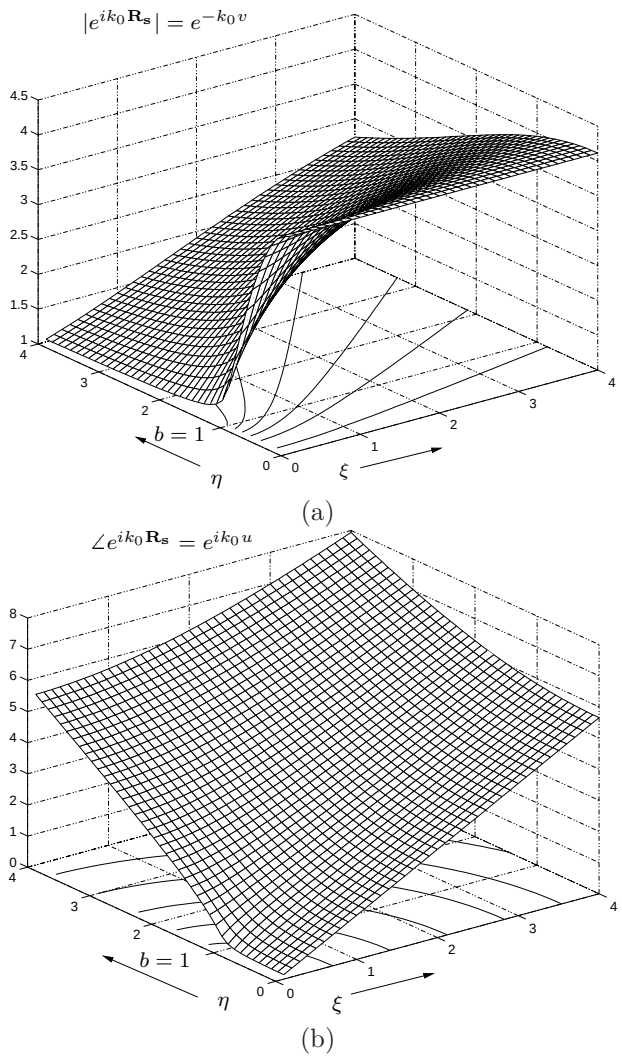

Figure 15. Exponential term, ET, contributions: (a) amplitude, and (b) phase.

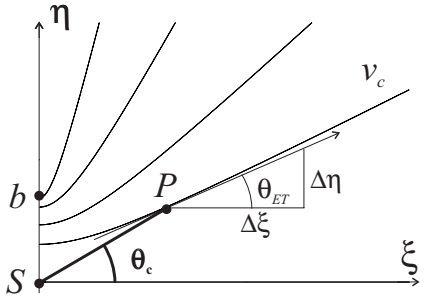

Figure 16. Complex angle definition $\boldsymbol{\theta}_c = \tan^{-1}(\eta/\xi - ib)$, and propagation direction of a field given by the exponential term, θ_{ET}. Conventional real angle is $\theta_c = \tan^{-1}(\eta/\xi)$.

As long as the maximum variation of the amplitude is orthogonal to the propagation direction, the perpendicular direction to $\Re\{\boldsymbol{\theta_c}\}$ provides with the information about the gradient of the field amplitude.

- **The imaginary part of the complex angle**, Figure 17b, provides with the information about how much the amplitude of the field varies in the direction of its maximum variation, and how much the phase of the field varies in the propagation direction. In Figure 18a and 18b, two differential length elements are defined in order to evaluate the amplitude and phase profiles, respectively. By calling

$$C_a = \frac{1}{amp(P)} \frac{|amp(P_1) - amp(P_2)|}{\Delta} = \frac{Ln\left(\frac{amp(P_1)}{amp(P_2)}\right)}{\Delta}, \tag{32}$$

and

$$C_p = \frac{phase(P_2) - phase(P_1)}{\Delta}, \tag{33}$$

it may be concluded that,

$$\Im\{\boldsymbol{\theta_c}\} = \text{ash}C_a = \text{ach}C_p. \tag{34}$$

- **Space of complex wavenumbers.** We can define, in the system of coordinates centered in the beam axis (ξ, η) the following magnitudes,

$$\begin{aligned} \mathbf{k}_\xi &= k_0 \sin\boldsymbol{\theta_c}, \\ \mathbf{k}_\eta &= k_0 \cos\boldsymbol{\theta_c}. \end{aligned} \tag{35}$$

Complex $\mathbf{k}_\xi$- and $\mathbf{k}_\eta$-spaces are obtained straight forward from $\sin\boldsymbol{\theta_c}$ and $\cos\boldsymbol{\theta_c}$ spaces. This fact opens the possibility to perform spectral decomposition analysis in terms of the complex wavenumber. For instance, the FT of the 2D free space Green's function, in (2),

$$\tilde{G}_f(k_\eta, \xi, b) = \frac{e^{i\sqrt{k_0^2 - k_\eta^2}(\xi - ib)}}{2i\sqrt{k_0^2 - k_\eta^2}}, \tag{36}$$

may be analytically continued into the complex wavenumber space as follows,

$$\tilde{G}_f(\mathbf{k}_\eta, \xi, b) = \frac{e^{i\sqrt{k_0^2 - \mathbf{k}_\eta^2}(\xi - ib)}}{2i\sqrt{k_0^2 - \mathbf{k}_\eta^2}}. \tag{37}$$

The SCW may be defined in an arbitrary reference system, no necessarily centered in the ξ-axis, as

$$\begin{aligned} \mathbf{k} &= k_0 \sin\boldsymbol{\theta}, \\ \mathbf{k} &= k_0 \cos\boldsymbol{\theta}. \end{aligned} \tag{38}$$

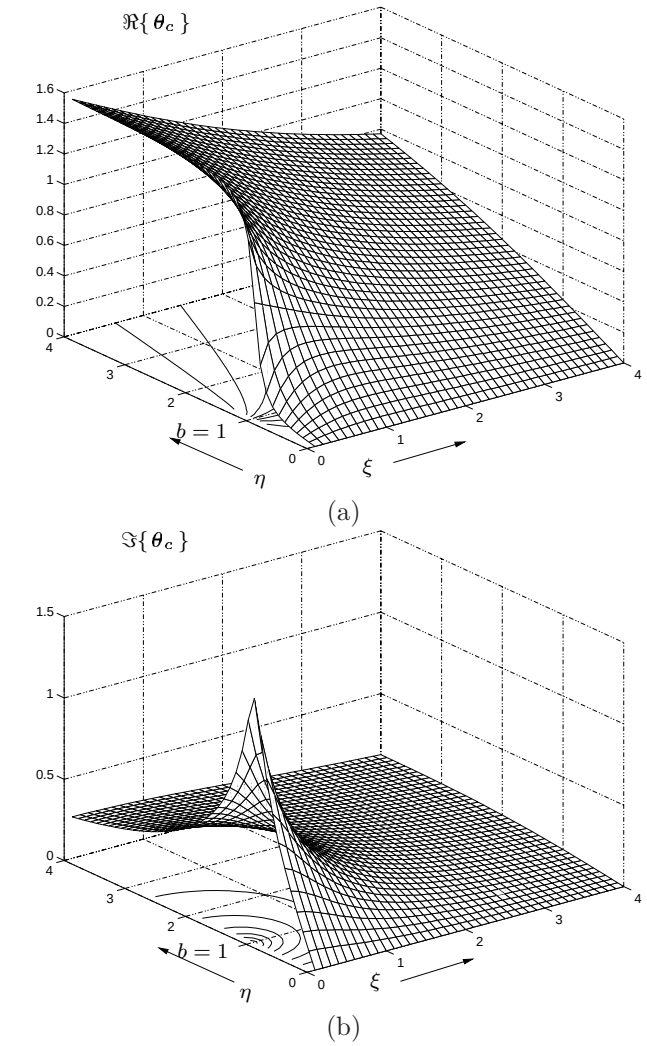

Figure 17. Complex angle $\boldsymbol{\theta}_c$ in the quadrant $(\xi \geq 0, \eta \geq 0)$: (a) real part of the complex angle, and (b) imaginary part of the complex angle.

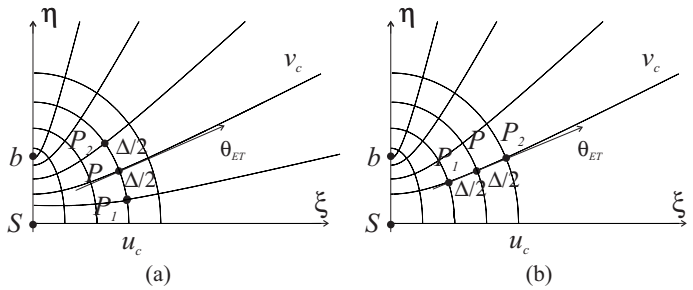

Figure 18. Differential length element definition to evaluate (a) the amplitude variation of the ET, and (b) the phase variation of the ET.

5. Conclusions

From the analytic continuation of the real coordinates of a 2D point source into the complex space, a new valid Green's function which leads to a more general representation of all the field solutions is obtained. Complex magnitudes such as complex distances, complex angles, and other associated complex functions arise from this formulation. Their complete parameterization provides a very valuable information concerning the analysis of the different particular solutions obtained from the general solution for the wave equation under analysis, once the solution has been analytically continued into the space of complex coordinates (complex beams in this particular study). Under this general consideration, some specific results should be emphasized.

Concerning the *space of complex distances* (and the related ones), the usual difficult problem associated to the parameterization of the range of validity of the different approximations that turns up the set of particular solutions, may be easily analyzed and understood in these complex domains. These parameterizations may then be translated and interpreted into the real propagation space. This methodology is able to provide a very clean and general initial representation of the whole problem by splitting the real space into a set of regions where each particular solution will be valid. Also, it will have a special relevance when considering the parameterization of the behavior of all the solutions, for instance, the set of solutions presented in Figure 2 for the specific radiation problem associated to complex beams under analysis in these papers. A particularly important application will be the use of these results in **Part II** to calibrate the boundaries associated to the different approximations, such as Gaussian beam paraxial or high frequency-far field approximations. Other important particular results applied to the complex beams problem will be the fact that the far field region may be validated in almost all the space, even at observation points very close to the real source location, Figure 7. Finally, as mentioned in the introduction, these initial representations of the whole problem will become even more important when applied to the analysis of scattering problems, such as those in [30].

Concerning the *space of complex angles* (and the related ones), it turns out that these magnitudes will play a fundamental role when trying to understand, in the real propagation space, specific scattering results such as the Snell complex law, the complex Bragg modes, complex rays, etc. In this sense, let us recall the interpretations associated to these complex magnitudes in Section 4: the real and imaginary parts of the complex angle provide with the information about the propagation direction and the amplitude variation of the field. Also, as cited in Section 4, the so called exponential term constitute the elementary field component for any 2D wave propagation, such as evanescent plane waves, which where formulated in terms of a complex angle, and maybe interpreted from the above mentioned guides, [4], formula. Another important aspect directly related to the space of complex angles discussion is the natural definition of complex wave numbers appearing from them. This natural definition suggested to the the authors the study of certain mathematical problems and their possible application to the representation of wave propagation phenomena; these problems will be associated to the representation of the sources in terms of complex Delta generalized functions, the analysis of the corresponding Green's functions, and also their complex spectral representation. If this generalization is possible (currently under study), it seems for the authors that all the analysis presented in this paper will be very important in order to understand this generalization, and also to translate all the results into the real propagation space.

Let us also mention that not only the complex beams problem may be formulated by using the complex methodology presented here. Other wave problems such as the *evanescent waves* already mentioned, as well as the *surface waves* problem turning out from the modified Helmholtz equation, and consequently from

the analytic continuation of the Green's function $K_0(k_0R) \rightarrow K_0(k_0\mathbf{R})$, may also be formulated in terms of complex distances and angles. The analysis of these particular problems may be found in [30].

Finally, the authors want to place emphasis on the fact that, even with all these initial parameterizations and analysis in mind, which are intended not only to facilitate the mathematical procedure, but also to clarify the real meaning of complex distances and angles, the last one continues being an obscure concept to be yet fully understood. The analysis presented in this paper suggests that, only when a *complex-polar description* (complex distances and angles together) may be performed, the full potential of these magnitudes will be reached. In the present two papers, the authors want to present what they think are only the first results that may provide the basis for future more general analysis.

List of Acronyms

Complex Spaces	
RPS	Real Propagation Space
SCD	Space of Complex Distances
SCA	Space of Complex Angles
STCA	Space of the Tangent of a Complex Angle
SSCA	Space of the Sine of a Complex Angle
SCCA	Space of the Cosine of a Complex Angle
SCW	Space of Complex Wavenumber
Field solutions	
CB	Complex Beam
NHCW	Non Homogeneous Cylindrical Wave
GB	Gaussian Beam
ET	Exponential Term of the NHCW
CW	Cylindrical Wave
EPW	Evanescent Plane Wave
Approximations	
CRC	Complex Radiation Condition
PC	Paraxial Condition
HF-FFC	High Frequency-Far Field Condition

List of Symbols

$\vec{r} \equiv (x, z)$	Real observation point vector
$\vec{r}_s \equiv (x_s, z_s)$	Real source position vector
$\vec{\mathbf{r}}_\mathbf{s} \equiv (\mathbf{x_s}, \mathbf{z_s})$	Complex source position vector
$R_s = \lvert\vec{r} - \vec{r}_s\rvert$	Real distance from the observation point to the real source location
$\mathbf{R_s} = \lvert\vec{r} - \vec{\mathbf{r}}_\mathbf{s}\rvert = u + iv$	Complex distance from the observation point to the complex source location
$\mathbf{R_s^2} \equiv \mathbf{z} = z_1 + iz_2$	Square of the complex distance
$1/\mathbf{R_s} \equiv \mathbf{w} = w_1 + iw_2$	Inverse of the complex distance
$\mathbf{n} \equiv x - \mathbf{x_s} = n_1 + in_2$	Complex difference of the x-coordinates of the real observation and complex source locations
$\mathbf{d} \equiv z - \mathbf{z_s} = d_1 + id_2$	Complex difference of the z-coordinates of the real observation and complex s source locations
$\boldsymbol{\theta} = \theta_1 + i\theta_2$	Complex angles
$\tan \boldsymbol{\theta} = t_1 + it_2$	Tangent of a complex angle

$\sin\boldsymbol{\theta} = s_1 + is_2$	Sine of a complex angle
$\cos\boldsymbol{\theta} = c_1 + ic_2$	Cosine of a complex angle
$\mathbf{k} = k_1 + ik_2$	Complex wavenumber
θ_{ET}	Real angle which describes the path direction of the ET
ρ_{CRC}	Parameter used to describe the error in the *CRC*
ρ_{PC}	Parameter used to describe the error in the *PC*
ρ_{HN}	Parameter used to describe the error when *HF-FFC* is applied to NHCW's
ρ_{HG}	Parameter used to describe the error when *HF-FFC* is applied to GB's

Acknowledgments

To Prof. Carlos Dehesa Martínez for his interesting and stimulating discussions and ideas regarding this paper. Some of the studies presented in this paper were supported by the Spanish CICYT under grant PB97-0487.

References

[1] A. Sveshnikov and A. Tikhonov, *The Theory of Functions of a Complex Variable.* MIR Publishers, Moscow, 1978.

[2] G. Deschamps and P. Mast, *Beam Tracing and Applications.* Proceedings of the symposium on quasioptics, pp. 379-395. Polytechnic Press, New York, 1964.

[3] G. Deschamps, *Gaussian Beam as a Bundle of Complex Rays.* Electronic Letters, Vol. 7, pp. 684-685, 1971.

[4] S. Choudhary and L. B. Felsen, *Asymptotic Theory for Inhomogeneous Waves.* IEEE Trans. on Ant. and Prop., Vol. AP-21, No. 6, pp. 827-842, November 1973.

[5] L. Felsen, *Complex Rays.* Philips Res. Repts 30, pp. 187-195, 1975.

[6] L. Felsen, *Ray Optical Techniques for High-Frequency Fields.* PPL Conference Publications, Polytechnic Institute of New York, USA 1976. Published by Southgate House, England, 1976.

[7] L. Felsen, *Complex-Source-Point Solutions of the Field Equations and their Relation to the Propagation and Scattering of Gaussian Beams.* Istituto Nazionale di Alta Matematica, Symposia Mathematica, Volume XVIII Bologna, 1976.

[8] S. Choudhary and L. Felsen, *Analysis of Gaussian Beam Propagation and Diffraction by Inhomogeneous Wave Tracking.* Proc. of the IEEE, Special Issue on Rays and Beams, Vol. 62, No. 11, pp. 1586-1598, November 1974.

[9] S. Shin and L. Felsen, *Inhomogeneous Wave Tracking in Anisotropic Media.* Proc. of the IEEE, Special Issue on Rays and Beams, Vol. 62, No. 11, pp. 1609-1610, November 1974.

[10] L. Felsen and S. Choudhary, *A New Look at Evanescent Waves.* Nouv. Rev. Optique, Vol. 6, No. 5, pp. 297-301, 1975.

[11] L. Felsen, *Evanescent Waves.* J. Opt. Soc. Am. Vol. 66, No. 8, pp. 751-760, August 1976.

[12] L. Bertoni, L. Felsen, and J. Ra, *Evanescent Fields produced by Totally Reflected Beams.* IEEE Trans. on Ant. and Prop., Vol. AP-21, No. 5, pp. 730-732, 1973.

[13] J. Arnold and L. Felsen, *Rigorous Asymptotic Theory of Evanescent Waves for Guided Propagation.* J. Acoust. Soc. Am. Vol. 67, pp. 757-763, 1980.

[14] J. Arnold and L. Felsen, *Rigorous Evanescent Wave Theory for Guided Modes in Graded Index Optical Fibers.* IEEE Trans. on Mic. Th. Tech., Vol. 28, No. 9, pp. 996-999, September 1980.

[15] P. Einziger and S. Raz, *On the Asymptotic Theory of Inhomogeneous Wave Tracking.* Radio Science, Vol. 15, No. 4, pp. 763-771, July-August 1980.

[16] P. Einziger and L. Felsen, *Evanescent Waves and Complex Rays.* IEEE Trans. on Ant. and Prop., Vol. 30, No. 4, pp. 594-604, July 1982.

[17] E. Heyman and L. Felsen, *Evanescent Waves and Complex Rays for Modal Propagation in Curved Open Waveguides.* SIAM J. of Appied Mathematics, Vol. 43, pp. 855-884, 1983.

[18] L. Felsen, *Rays, Modes and Beams in Optical Fibre Waveguides.* J. Opt. Soc. Am. Vol. 66, No. 8, pp. 751-760, August 1976.

[19] J. Maciel and L. Felsen, *Gaussian Beam Analysis of Propagation from an Extended Plane Aperture Distribution Through Dielectric Layers, Part I-Plane Layer.* IEEE Trans. on Ant. and Prop., Vol. 38, No. 10, pp. 1607-1617, October 1990.

[20] J. Maciel and L. Felsen, *Gaussian Beam Analysis of Propagation from an Extended Plane Aperture Distribution Through Dielectric Layers, Part II- Circular Cylindrical Layer.* IEEE Trans. on Ant. and Prop., Vol. 38, No. 10, pp. 1618-1624, October 1990.

[21] S. Shin and L. Felsen, *Multiple Reflected Gaussian Beams in a Circular Cross Section.* IEEE Trans. on Mic. Th. and Tech, Vol. 26, No. 11, pp. 845-851, November 1978.

[22] A. Green, H. Bertoni, and L. Felsen, *Properties of the Shadow Cast by a Half-Screen When Illuminated by a Gaussian Beam.* J. Opt. Soc of Am., Vol. 69, No. 11, pp. 1503-1508, November 1979.

[23] E. Kriezis, P. Pandelakis, and A. Papagiannakis, *Diffraction of Gaussian Beam from a Periodic Planar Screen.* J. Opt. Soc. Am. A, vol.11, No. 2, September 1990.

[24] E. Heyman and L. Felsen, *Gaussian beam and pulsed-beam dynamics: complex-source and complex-spectrum formulations within and beyond paraxial asymptotics.* J. Opt. Soc. Am. A, Vol. 18, No. 7, pp. 1588-1611, 2001.

[25] M. González Morales and E. Gago-Ribas, *On the Application of the Analytical Continuation to EM Fields.* The Fifth International Symposium on Antennas, Propagation ans EM Theory, ISAPE'2000, pp. 61-64. China, August 2000.

[26] E. Gago-Ribas, M. González Morales, and C. Dehesa Martínez, *Analytical Parametrization of a 2D Real Propagation Space in Terms of Complex Electromagnetic Beams.* Special Issue on Electromagnetic Theory-Scattering and Diffraction, IEICE Transactions on Electronics, Vol. E80-C, No.11, pp. 1434-1439, Japan, November 1997.

[27] M. González Morales and E. Gago-Ribas, *Inhomogeneous Cylindrical Waves: an Approach to Complex Beams.* IEEE AP-S International Symposium, Vol. 2, pp. 1396-1399. Orlando, USA., July 1999.

[28] M. González Morales and E. Gago-Ribas, *High Frequency-Far Field Conditions for Complex Source Fields.* Millenium Conference on Antenas and Propagation, pp.25. Davos, Switzerland, April 2000.

[29] E. Gago-Ribas and M. González Morales, *Complex Distances and Complex Angles in Beam Propagation and Scattering.* 4th Conference on Electromagnetic and Light Scattering bt Nonspherical Particles. Theory and Applications, pp. 103-110. Vigo, Spain., September 1999.

[30] M. González Morales, *Espacios Complejos. Aplicación a Problemas de Radiación y Dispersión Electromagnética de Haces.* Ph. Dissertation. Universidad de Valladolid, 2001.

[31] M. González Morales and E. Gago-Ribas, *Complex Space Beam Analysis of Scattering Problems: A First Example.* URSI International Symposium on EM Theory. Canada, May 2001.